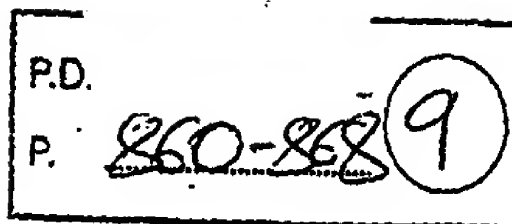


XP-001073846



Electrochemical Noise Resistance as a Tool for Corrosion Rate Prediction

G. Gusmano, G. Montesperelli, S. Pacetti, A. Petitti,* and A. D'Amico**

ABSTRACT

Current and potential fluctuations (electrochemical noise [EN]) between two nominally identical carbon steel electrodes were recorded in a solution of sodium phosphate (Na_3PO_4) at different concentrations. After passivation was reached, pitting was induced by addition of chlorides. Data were collected with different sampling rates. Linear polarization resistances (LPR) also were measured. Electrochemical signals were transposed in the frequency domains using the fast Fourier transform. Statistical parameters from the signals in the time and in the frequency domains were compared with corrosion rates (V) as measured by LPR. Noise resistance (R_n) also was calculated. From standard deviation (σ) values of the current and potential noises, pitting attack was revealed at its onset. Good correlation between data from the different techniques was found. R_n gave values proportional to the polarization resistance (R_p). The issue of how sampling rate can affect EN data collection also was addressed.

KEY WORDS: carbon steel, corrosion rate, current, electrochemical noise, fast Fourier transform, linear polarization resistance, passivation, pitting, potential, sampling rate, type 1040 carbon steel

INTRODUCTION

All corrosion processes — general corrosion, pitting attack, crevice corrosion, and stress corrosion cracking (SCC), as well as passive film buildup — cause spontaneous fluctuations of the free-corrosion potential of the electrodes. These fluctuations are termed electrochemical noise (EN), and their analysis is used widely in the examination of different corrosion processes.¹⁻¹⁰ Although interest in EN analysis has increased in corrosion studies over the past 15 years, some doubt remains on the correlation between the occurring phenomenon and the signal generated. From a qualitative point of view, it has been reported that values of statistical parameters of EN, such as standard deviation (σ) and the root-mean-squared (rms) values of the potential, can represent the corrosion status of the metal and permit identification of the nature of attack.^{1-2,11} Some tentative correlations between σ and the corrosion parameters (corrosion current and polarization resistance [R_p]) have been proposed,^{4,6,12} but their application seems not to be so general. In the last few years, interest in the current noise has grown. The study of the current fluctuations between corroding electrodes seems to be more significant than potential studies.⁷⁻⁸ More recently, use of the noise resistance (R_n) as calculated from potential and current noise data was proposed to be equivalent to R_p .¹³⁻¹⁷ Much discussion can be found in the literature on this topic, and a deeper analysis is required.

A powerful analysis of EN acquisitions can be performed by transposing data in the frequency do-

Submitted for publication April 1996; in revised form, December 1996. Presented in part as paper no. 336 at CORROSION/96, March 1996, Denver, CO.

* University of Rome, Tor Vergata, Department of Chemical Sciences and Technologies, Via della Ricerca Scientifica, 00133, Rome, Italy.

** University of Rome, Tor Vergata, Department of Electronic Engineering, Via della Ricerca Scientifica, 00133, Rome, Italy.

main. A traditional tool that provides this transformation is the fast Fourier transform (FFT).¹⁸⁻¹⁹ FFT performs a spectral analysis of the random transient of the EN signal in a frequency range dependent upon sampling time and length of the data recording. Results of the spectral analysis commonly are given as the decibel (dB) of rms current or potential vs frequency on a logarithmic scale, resulting in the power spectral density (PSD) plot. Some authors have found a relationship of $1/f$ between the measured noise power and the frequency.^{2,20-21} This seems an oversimplification of the problem, since every phenomenon occurring at the electrodes can result in an additional slope on the PSD plot. The presence of a capacitance resulting, for example, from a film formation or a diffusion element can increase the slope in the PSD plot from 20 dB/decade to 30 dB/decade.²

Generally speaking, an $f^{-\alpha}$ dependence would be more realistic, where α is different from unity.

Moreover, the power level of the signal as calculated from the PSD in the frequency-independent region, seems related to the corrosion rate (V_c).¹¹ According to some authors, other transformation analyses, such as the maximum entropy method (MEM), give the advantage of minor scattering of the data with respect to FFT.^{4,22} Recently, Roberge published results of a statistical analysis of EN data based upon the stochastic process detector (SPD) method.²³ This analysis offers a new approach to the EN interpretation problem based upon the stochastic process mechanics.

Many theoretical analyses of EN can be found in the relevant literature. The starting point is the study of the faradaic noise associated with electrochemical reactions.²⁴⁻²⁵ Validity of these models is within the limits of small deviations from the equilibrium state. Some advanced studies take into account the EN associated with the induction period of pitting and related to the adsorption/desorption processes of halide ions on the passive metal surface.²⁶⁻²⁹

The objective of the present work was to give an evaluation of further potentiality of this technique, illustrating the advantage of using EN resistance instead of the current and potential noise and the influence of sampling time on the significance and the reliability of data collection. Tests were carried out on mild steel specimens in passivating conditions and under pitting attack. Results of EN analysis in the time and frequency domains were compared with V_c as measured using the linear polarization resistance (LPR) method.

EXPERIMENTAL

Measurements were performed using a commercial LPR probe with three electrodes. The cylindrical electrodes, 4 mm (0.16 in.) in diameter and 24 mm

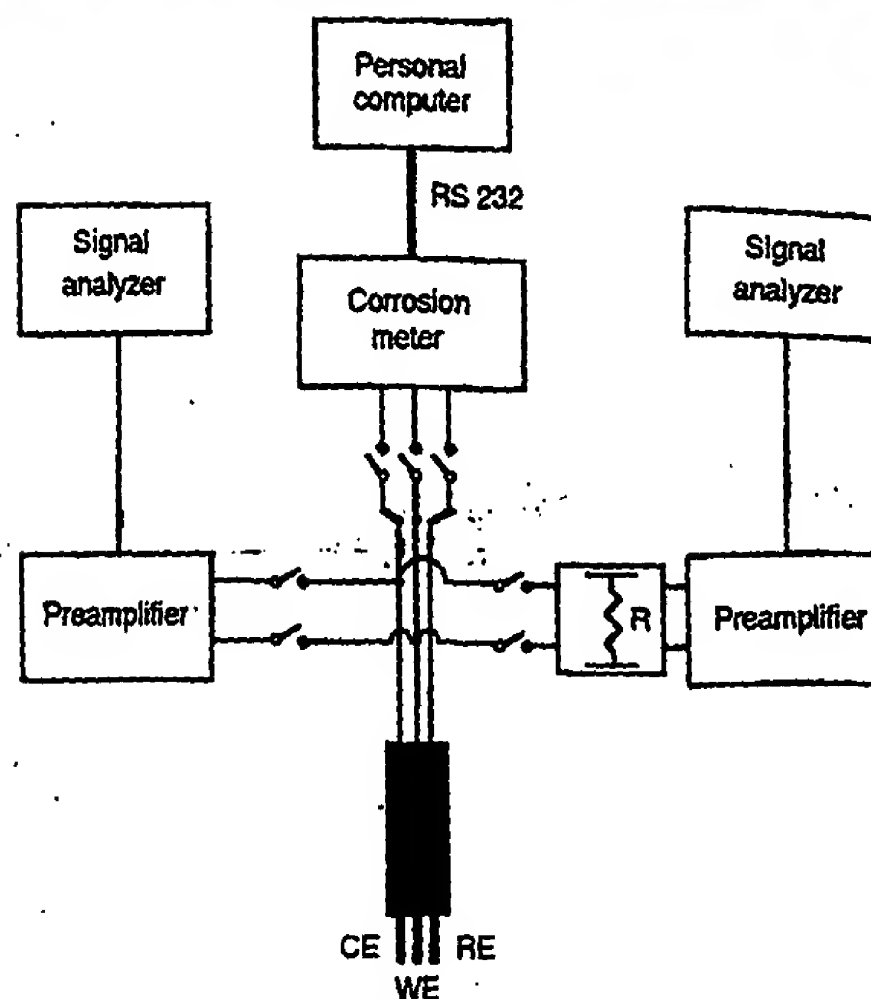


FIGURE 1. Scheme of measuring apparatus.

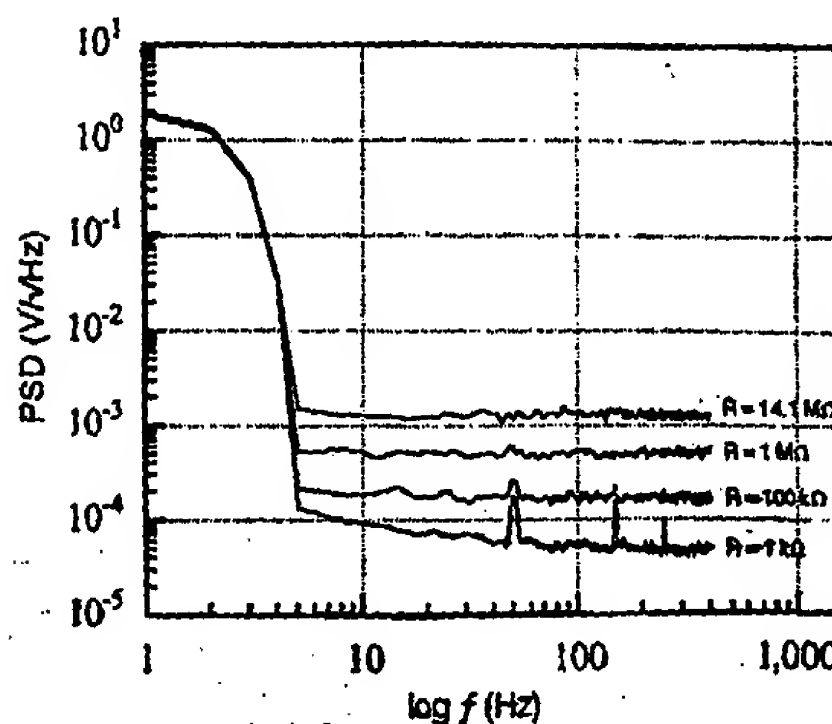
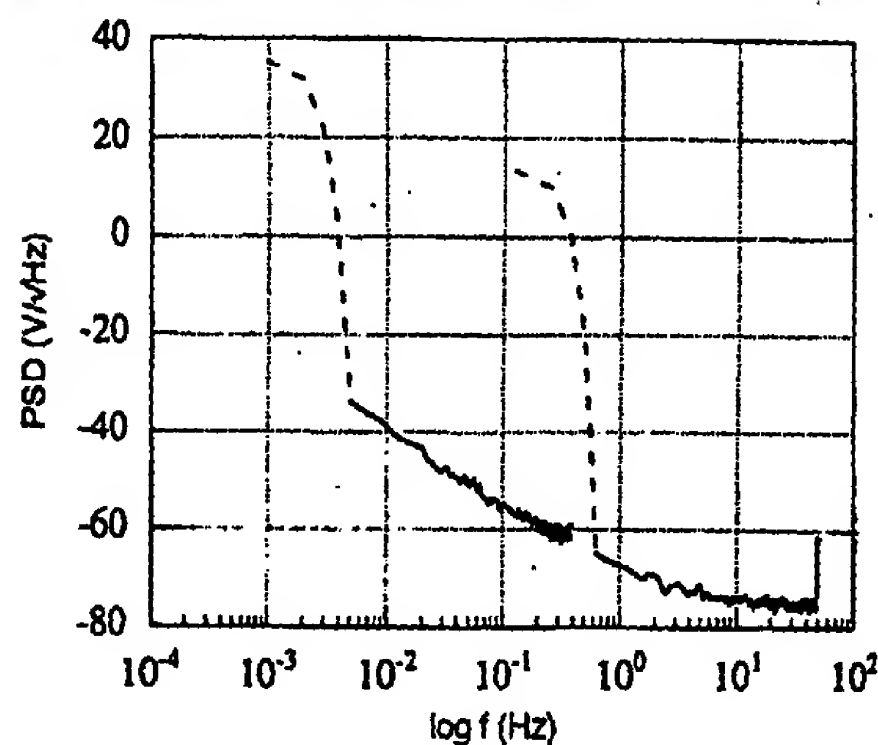


FIGURE 2. PSD of the potential noise related to R .

(0.96 in.) long (total exposed area = 3 cm² [0.49 in.²]) were fabricated from type 1040 (UNS G10400)⁽¹⁾ carbon steel. Before testing, the electrodes were polished by grinding with 500- through 1,200-grade abrasive papers, washed in distilled water, washed in acetone, and then dried in air.

During the tests, the electrodes were immersed fully in the solution. Visual inspections of the electrodes were made during the tests. At the end of each test, the electrodes were inspected using a stereo microscope.

⁽¹⁾ UNS numbers are listed in *Metals and Alloys in the Unified Numbering System*, published by the Society of Automotive Engineers (SAE) and cosponsored by ASTM.

FIGURE 3. PSD of the same R in two different frequency range.

All tests were carried out in solutions prepared using reagent-grade chemicals. The passivating agent was 50 mM, 20 mM, or 5 mM sodium phosphate (Na_3PO_4) to generate a wide range of passivation. Breakdown of the passive film was induced by adding a sodium chloride (NaCl) concentrated solution to obtain a chloride concentration of 0.34 M. All solutions contained 20 mM sodium perchlorate (NaClO_4) to minimize solution resistivity. During immersion into the passivating test solution, formation and growth of the passive film were studied by recording V_e and potential and current noise as a function of immersion time. The same measurements were performed after addition of the chloride solution. All measurements were carried out at room temperature.

Electrochemical potential noise was recorded using an Hewlett Packard 35665A[†] dynamic signal

[†] Trade name.

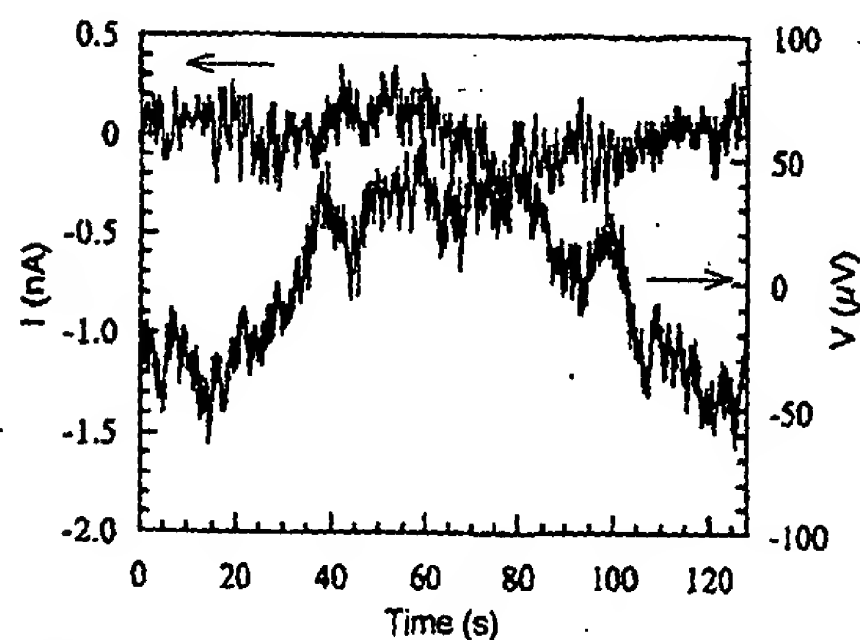
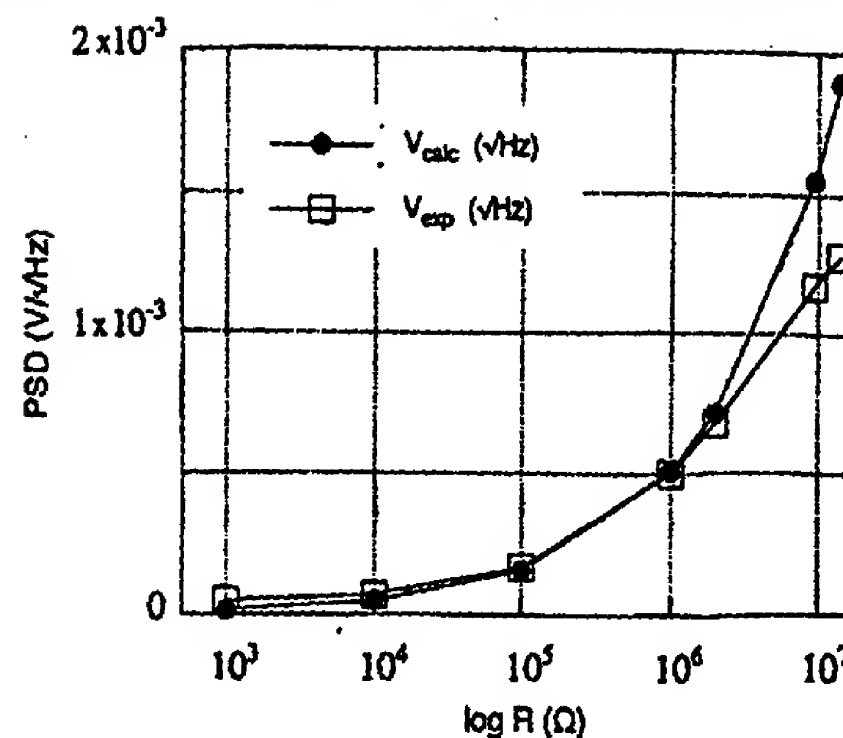


FIGURE 5. Time record of current and potential noise after 9 h of immersion in a 5 mM phosphates solution.

FIGURE 4. Comparison between theoretical and experimental potential noise as a function of R .

analyzer coupled, when required, with an EG&G PARC 5113[†] low-noise preamplifier. The signal analyzer had a sensitivity < -140 dBV_{rms}/Hz and an accuracy of $\pm 2.92\%$ (0.25 dB) of the measurement. The preamplifier resulted in a circuit-noise level, referred to the input, of < 4 $\mu\text{V}/\sqrt{\text{Hz}}$ at 1 kHz.

Electrochemical current noise was recorded using the same signal analyzer and inserting a parallel reference resistance (R) between the probe and the preamplifier. Values of R were chosen to be of the same order of magnitude as the total resistance of the system, as estimated by electrochemical impedance spectroscopy (EIS) measurements carried out through preliminary tests, to have the maximum transfer of noise power.

Potential and current fluctuations were recorded between the working (WE) and the counter (CE) electrodes of the LPR probe (Figure 1). Different data sets of 1,024 readings were recorded at sampling frequency

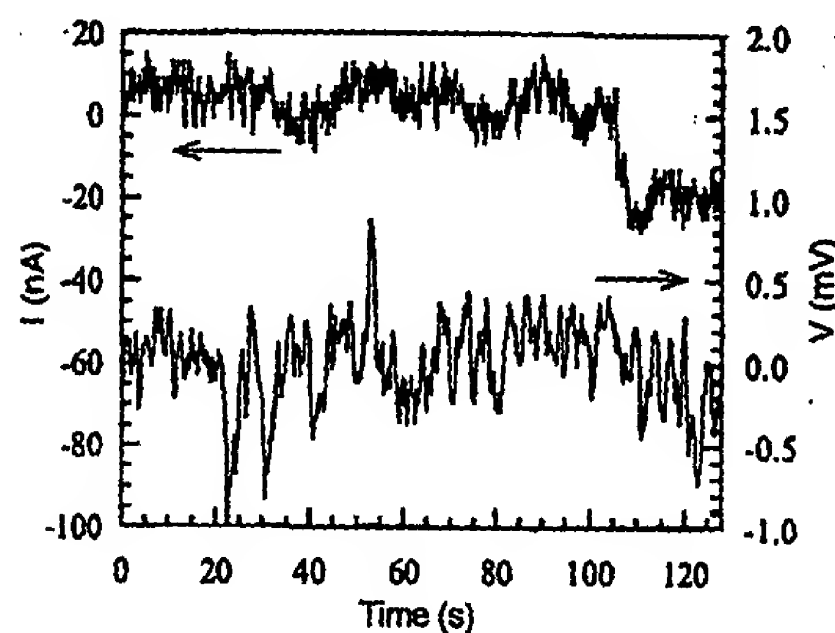


FIGURE 6. Time record of current and potential noise after 8 h from the chloride addition (same test of Figure 5).

cies of 2 Hz, 8 Hz, or 32 Hz. During the current EN recording, the CE and WE were coupled across the preamplifier, which had a resistance in parallel. Then, the electrodes were uncoupled and immediately coupled again across the preamplifier to record the potential EN. After data collection, the linear trend component was estimated by the least-squares method³⁰ and then eliminated by subtraction.

The statistical calculations and analysis (for and frequency distribution), as well as the linear fit by the least-squares method, were performed using commercial software.

R_p was calculated by:¹⁵⁻¹⁶

$$R_p = \frac{\sigma_v}{\sigma_i} \quad (1)$$

where σ_v and σ_i are the standard deviations of potential and current EN. All potential and current noise data collected in the time domain were transformed in the frequency domain through the FFT method, performed online by the signal analyzer.

V_e and R_p were measured using an ADSE¹ digital corrosion meter connected to a personal computer and managed by dedicated software. The corrosion meter used a three-electrode method. Polarization was 10 mV, and the scan rate was 0.1 mV/s. The value of the Tafel slope (b_a and b_c) used by the software to calculate V_e was 120 mV. Calibration of the corrosion meter was carried out on the same electrodes in solution with different corrosiveness, using the mass-loss method. Good agreement was found. V_e measurements were performed immediately after each set of current and potential noise acquisition by connecting the probe to the corrosion meter. All V_e data were averaged through at least four measurements. Preliminary tests showed the influence of the LPR measurements on the EN recording. For this reason, in each set of data collection, the LPR were performed after the acquisition of EN. In the subsequent set, usually performed after an hour from the previous, no residual effect due to LPR measurement was observed on EN. Commercial corrosion meters commonly used give V_e values referred to the total electrode area. For this reason, it was decided to use the data as obtained from the instrument. Taking into account that the measurements (LPR and noise) were carried out exactly on the same electrodes, the comparison between results coming from the different techniques was independent of the absolute value.

To calibrate the signal analyzer, some preliminary tests were carried out with different R (values ranging from 1.0 k Ω to 14.1 M Ω). The PSD of the potential noise associated to the temperature-induced fluctuations (Johnson noise) are reported in Figure 2. Each signal was averaged through 60 data

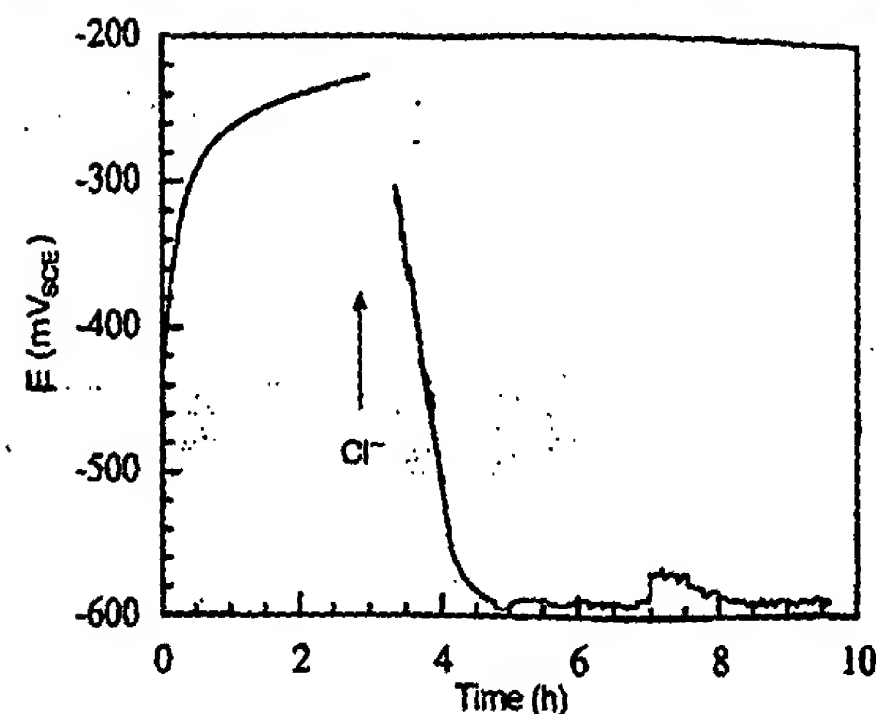


FIGURE 7. Open-circuit potential for a test in a 20 mM phosphates solution.

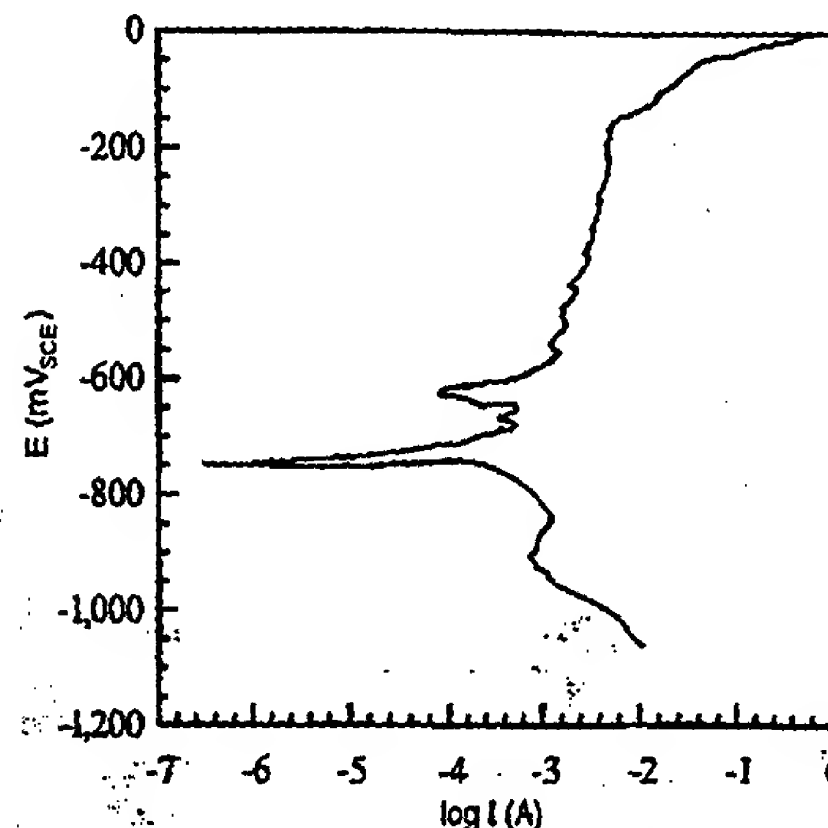


FIGURE 8. Linear polarization curve for the same test as Figure 7, collected 1 h after chloride addition.

acquisitions, and the gain of the preamplifier was fixed at 4,000.

The PSD spectra were characterized by a sudden decrease of the power level at low frequencies and a 1/f trend at high frequencies. To better clarify the nature of the first part of the plot, further tests were carried out on the same R (100 k Ω) in different frequency ranges. Results are reported in Figure 3. The same strong decrease of the power level was observed. Except for the first five points (dotted lines in Figure 3), the spectrum taken at the lowest frequency range perfectly continued the plot at the highest frequency range. This proved that the first five points resulted from an instrumental artifact. For this reason, they were neglected in elaboration of the experimental data.

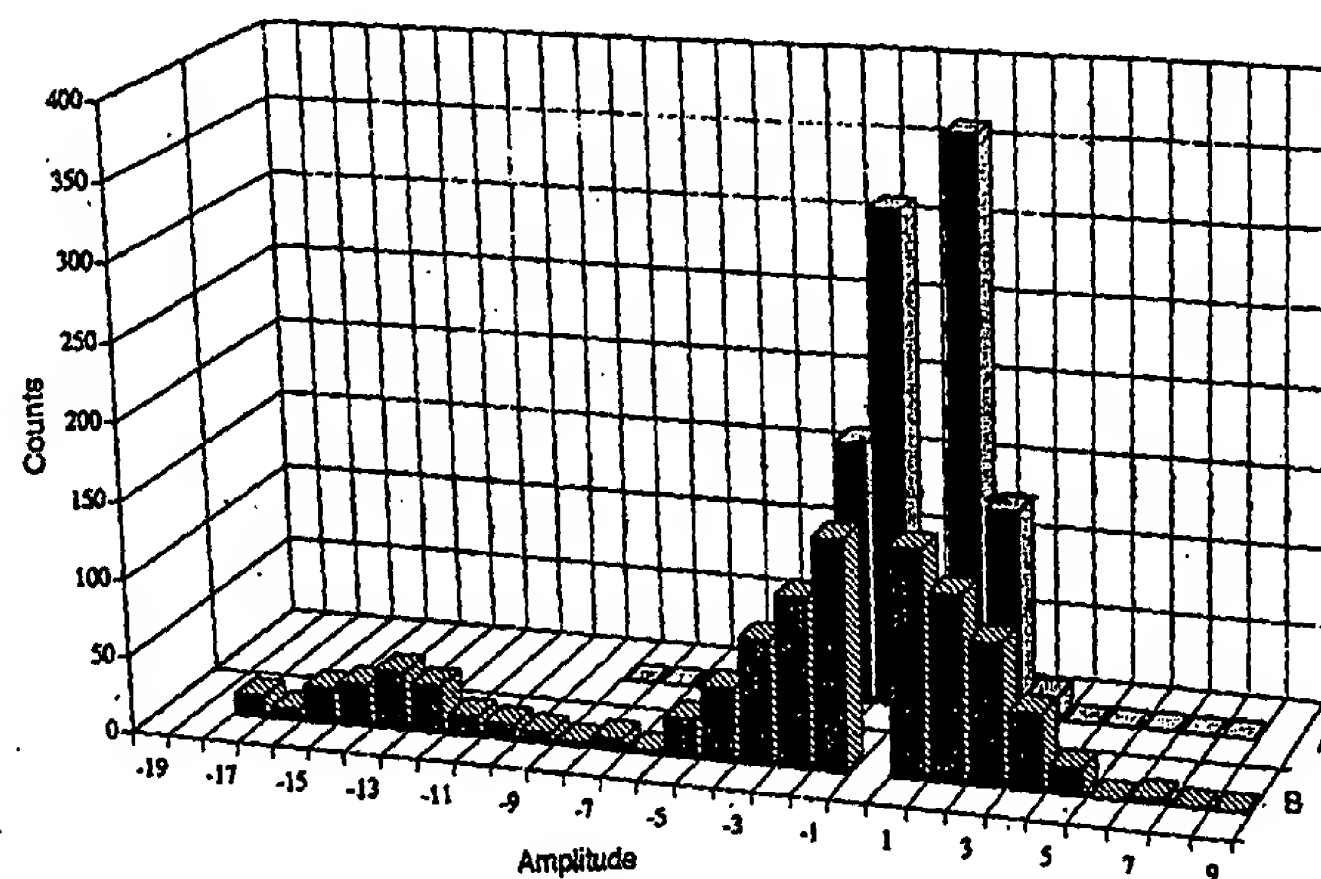


FIGURE 9. Histogram representation of current noise data of Figures 5 and 6: (A) after 9 h of immersion in the passivating solution and (B) 8 h after chloride addition.

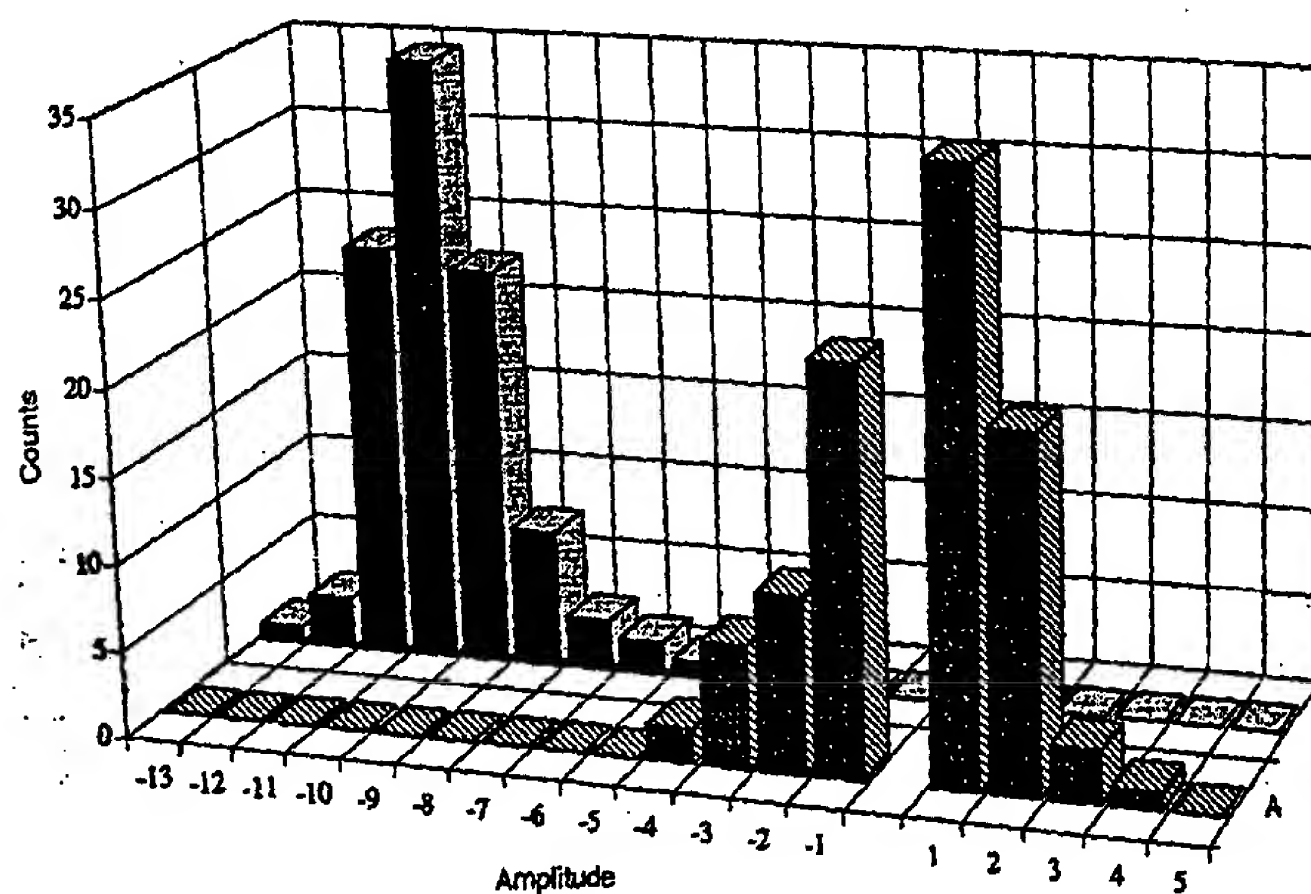


FIGURE 10. Histogram representation of: (A) the first and (B) the last 100 points of the current signal of Figure 6.

The noise power level of the signal at high frequencies of the spectra of Figure 2 was compared to the rms value of theoretical noise, as calculated in the arbitrary bandwidth (Δf) by the Nyquist relationship:³¹

$$\bar{V}_n^2 = 4kRT\Delta f \quad (2)$$

where \bar{V}_n^2 is the mean square noise voltage, k is the Boltzmann's constant, and T is the absolute tem-

perature of R . Results are summarized in Figure 4. In the range of the total impedance of the system (80 k Ω as maximum value measured in preliminary tests), the difference between experimental and theoretical potential noise appeared to be negligible.

RESULTS AND DISCUSSION

Figures 5 and 6 show the current and potential fluctuations recorded after 9 h of immersion into the passivating solution (5 mM phosphates) and after 8 h

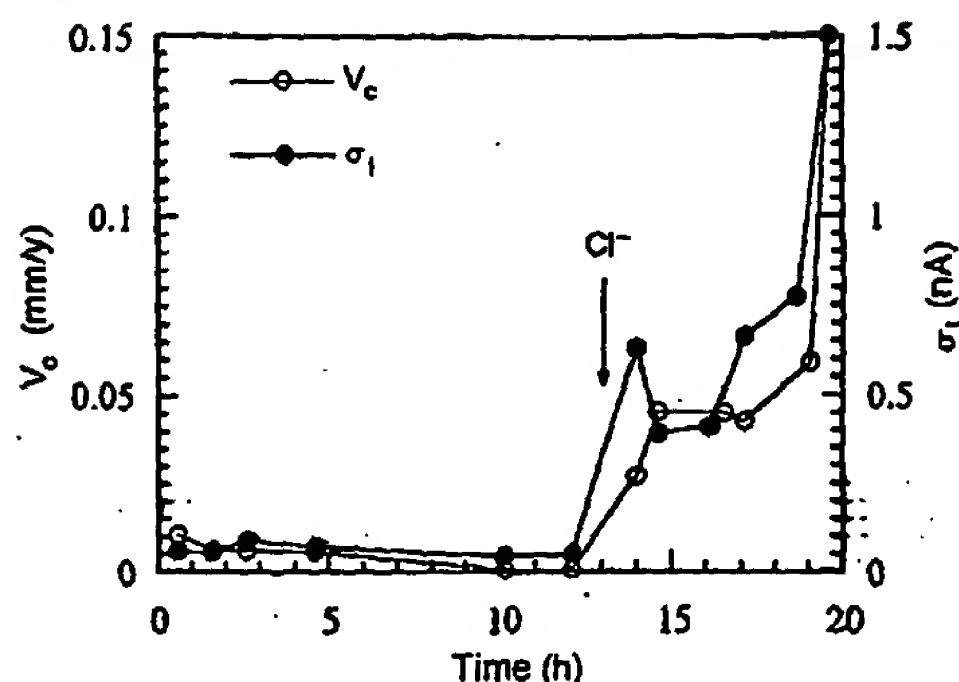


FIGURE 11. Comparison between σ of the current data and V_e vs immersion time for a 20 mM phosphate solution.

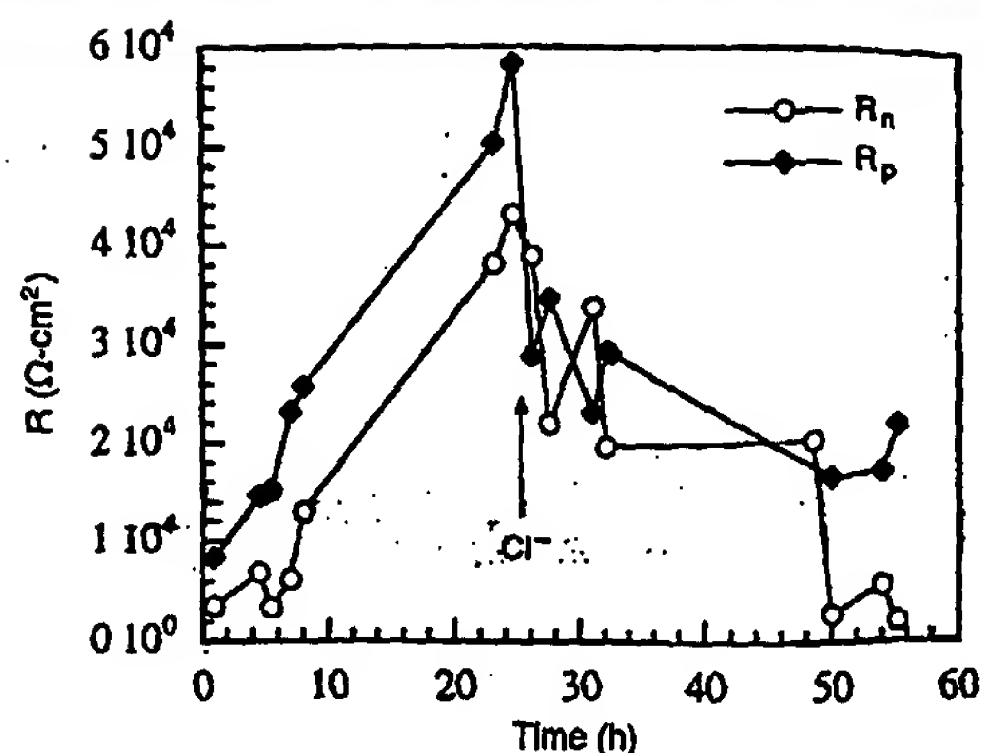


FIGURE 12. Comparison between R_n and R_p vs immersion time for a 50 mM phosphate solution.

from the addition of chlorides, respectively. The sampling frequency was 8 Hz.

In the case of complete passivation (Figure 5), the current and potential EN were characterized by small fluctuations. Values of σ were 0.13 nA and 30.50 μ V. V_e in the same interval of time was 1.5 μ m/y (0.06 mpy).

Pitting attack caused by the addition of chlorides produced an increase in fluctuation amplitudes and in σ (9.81 nA and 250 μ V) of both signals. V_e increased up to 240 μ m/y (9.4 mpy) as referred to the total electrode area. Taking into account the pit area estimated by microscopic observation after the test, V_e was 1.6 mm/y.

The pitting occurrence was confirmed by visual observation and by recording the trend of the open-circuit potential as reported in Figure 7. The occurrence of pitting also was confirmed by polarization curves performed at the end of the passivation period and after addition of chlorides. Figure 8 shows the polarization curve collected 1 h after the addition of chlorides. Visual inspections after each test showed no evidence of crevice corrosion.

As a general trend, in all tests performed, σ values of 0.5 nA and 50 μ V or less were characteristic of a good passivation state. A more clear representation of evaluation of the corrosion phenomena is given in Figure 9, in which the current data of Figures 5 and 6 were sorted in a distribution of population. Because of the dramatic differences of corrosion events in the passive state and during pitting attack and the very large difference in the data distribution, the bin amplitude was chosen differently in the two histograms: 0.125 nA for Histogram A and 1.785 nA for Histogram B. In the Z axis, the number of counts is reported.

The histogram related to the passivated electrodes (Histogram A) showed a very sharp Gaussian distribution. The data related to pitting condition

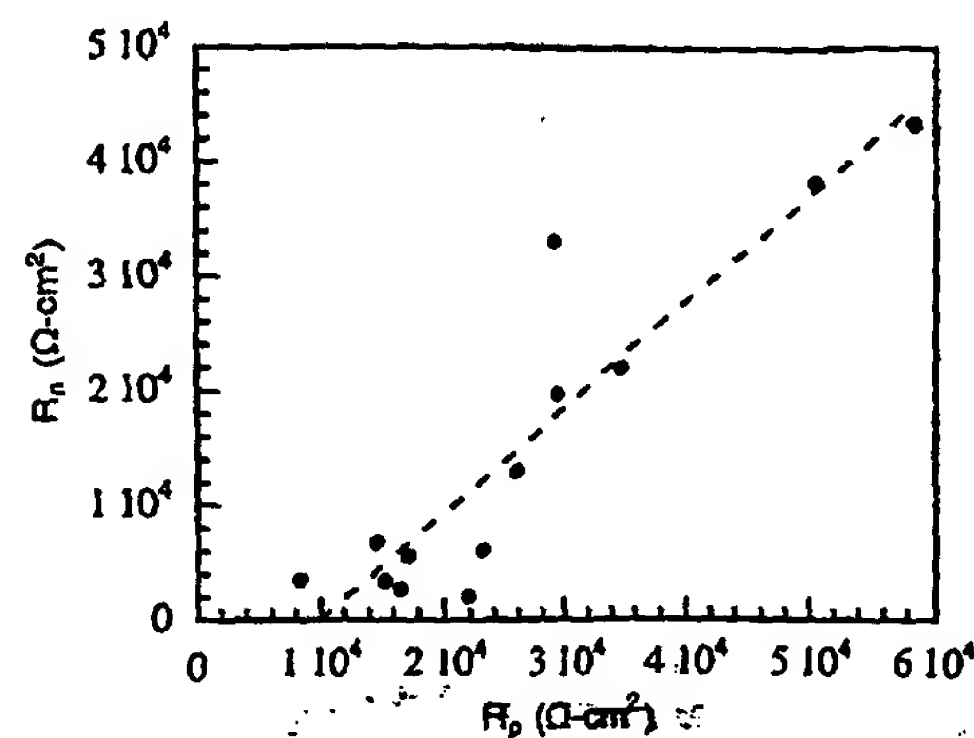


FIGURE 13. Correlation between R_n and R_p .

(Histogram B) showed a bimodal distribution with two populations both characterized by broad gaussian curves. This bimodal behavior resulted from the final part of the time recording in which, after a steep variation (at ~ 105 s), the signal fluctuated around a new average value as can be observed by plotting the distribution of population of the first and the last 100 points of Figure 6, respectively. Histograms A and B of Figure 10. The sudden variation of the signal probably was representative of the initiation and propagation of a pit on one of the electrodes that caused a predominant anodic behavior of that electrode with respect to the other.

As a general trend, σ of the EN signals followed the variation in solution corrosiveness. A typical trend of a whole test is reported in Figure 11 for the current EN.

From the ratio of σ of the potential and the current EN, R_n was obtained and compared with R_p as a

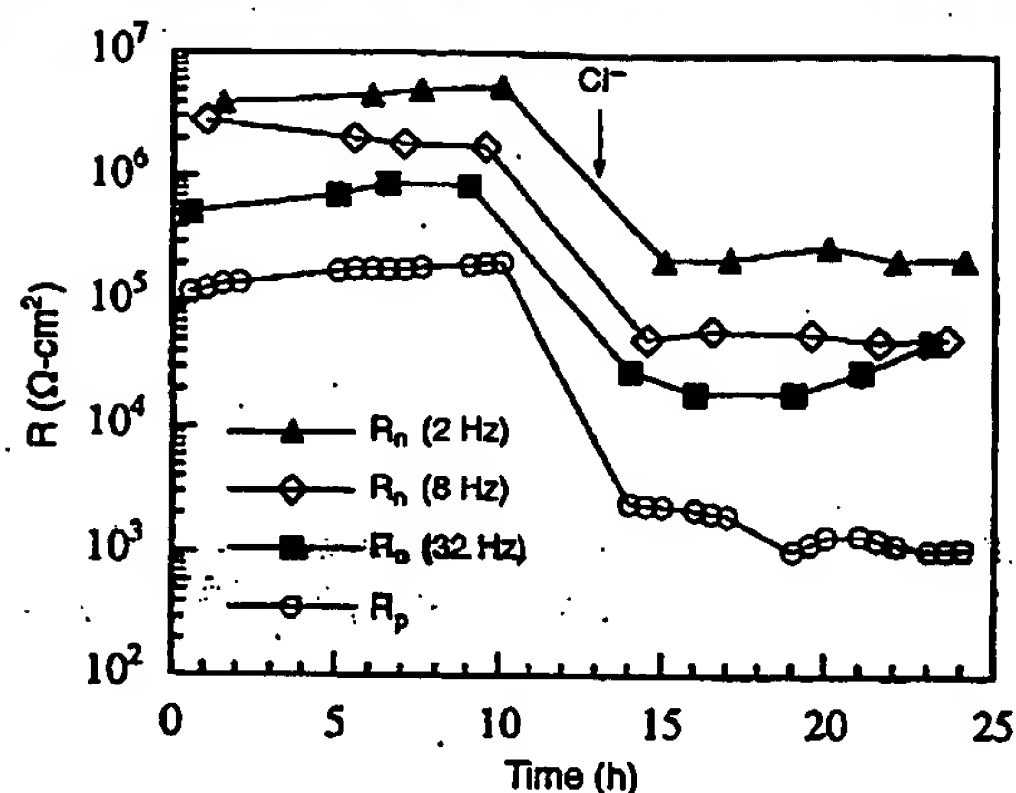


FIGURE 14. Comparison between R_n and R_p obtained with different sampling frequencies as a function of immersion time for a 5 mM phosphate solution.

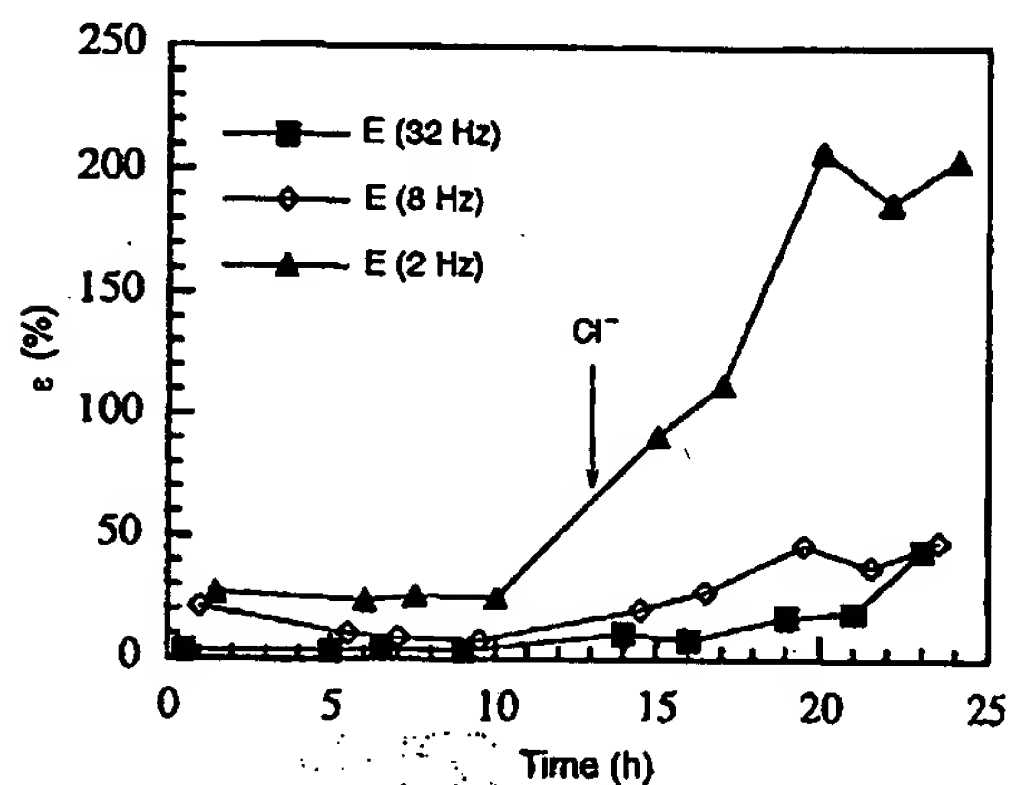


FIGURE 15. Representation of relative errors calculated for different sampling times as a function of immersion time.

function of immersion time. Good agreement was found, as shown in Figure 12 for a test in a 50 mM phosphate solution. R_p and R_n variations were within the same order of magnitude. Figure 13 shows the correlation between R_p and R_n . The dotted line indicates the linear fit as obtained by the least-squares method. The correlation coefficient was $R = 0.92$. The results demonstrated the strict correlation between R_p and R_n , both promoted by a charge-transfer reaction. The difference in the absolute resistances could be attributed to the different measurement technique. In LPR measurements, R_p was measured by applying an external polarization of 10 mV to the WE, while in EN measurements, R_n was obtained by very small potential fluctuation (from 100 μ V to 1 mV). This condition guaranteed better linearity between current and potential.

To evaluate the influence of sampling time on the EN data, several tests were performed using different sampling frequencies.

An example is given in Figure 14, where the values of R_n corresponding to acquisition frequencies of 2 Hz, 8 Hz, or 32 Hz are compared to values of R_p as a function of immersion time. The increase of sampling frequency caused a decrease in the difference between R_n and R_p . In Figure 15, data of Figure 14 are plotted in terms of relative difference of R_n with respect to R_p for different sampling frequencies. Relative differences were calculated according to:

$$\varepsilon = \frac{\sqrt{(R_n - R_p)^2}}{R_p} \quad (3)$$

The difference increased with decreasing the sampling frequency and moving from passivation to the pitting condition. A pronounced increase of the relative difference was observed for the curve relative to a sampling frequency of 2 Hz and was more evident after the chloride addition. The choice of a correct sampling frequency seemed to be fundamental for reliability of the noise acquisitions.

This behavior could be explained by the fact that the electrochemical phenomena at shortened acquisition times could be considered stationary with a better approximation. This seemed to be an experimental confirmation of the stationary assumption required for a correct R_n calculation, as reported by Blerwager.¹⁶ Moreover, the intrinsic nature of the passive state better approximated a steady-state condition than pitting attack.

Figures 16 and 17 present the PSD recorded after 10 h of immersion in a passivating solution (5 mM phosphates) and 9 h after the addition of chlorides, respectively. The sampling frequency was 2 Hz.

According to some authors, a dependence between the power level of the signal and the frequency has been found in the frequency region between 0.01 Hz and 0.1 Hz.³²⁻³³ As shown in Figure 16, formation of the passive film on the electrodes surfaces produced a slope of 32.8 dB/decade in the potential noise and 24.1 dB/decade in the current noise. After addition of chlorides (Figure 17), the slope decreased to 16.4 dB/decade in the potential spectrum.

As a general trend, slopes of ≤ 20 dB/decade in the potential spectrum were indicative of pitting corrosion, while a roll-off of > 20 dB/decade characterized a passive state. These findings were in agreement with data reported in the literature.^{32,34}

The current PSD did not show significant differences in the slope in the two conditions.

More relevant findings were obtained by analyzing data in the high-frequency region (> 0.1 Hz) in which the power level was independent of the frequency. In fact, data calculated from this frequency

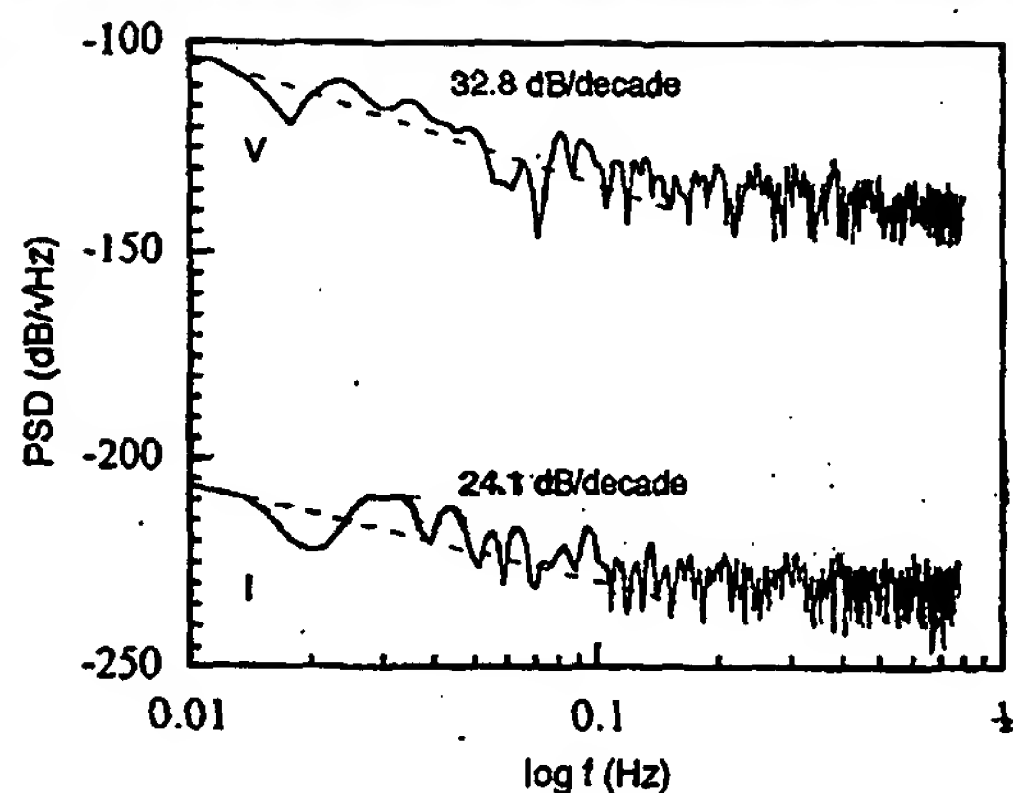


FIGURE 16. Potential and current PSD recorded after 10 h of immersion in 5 mM phosphate solution.

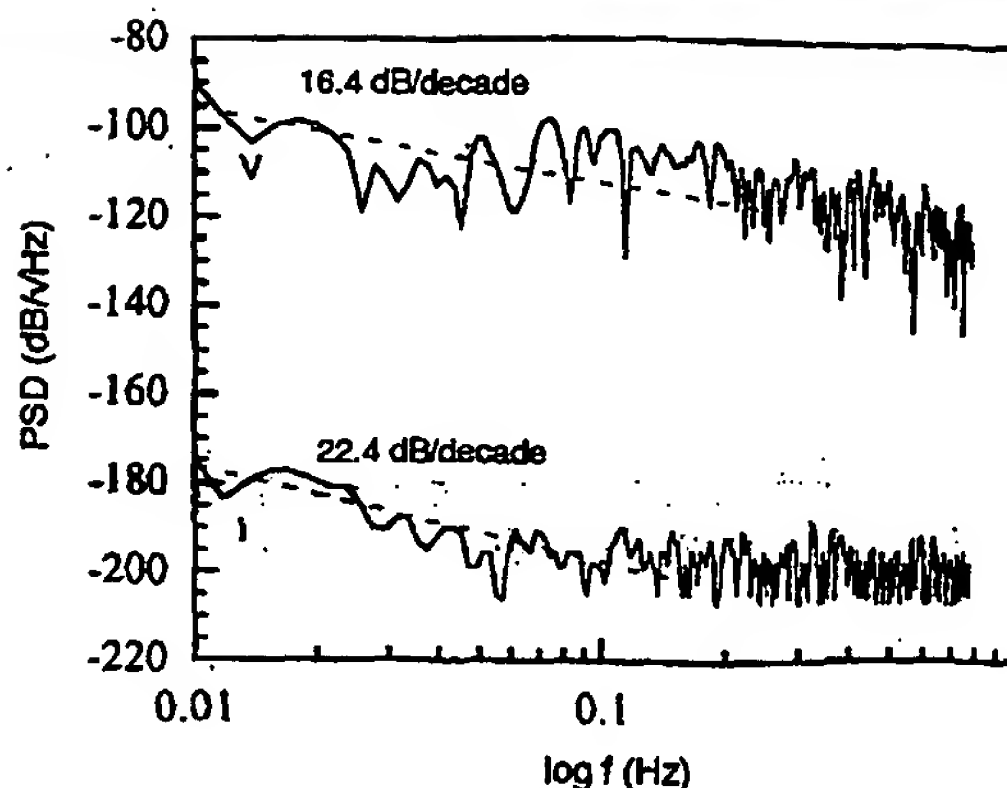


FIGURE 17. Potential and current PSD recorded 9 h after chloride addition (same test as Figure 16).

region seemed less subjected to random differences if different data collections coming from the same test were considered. This finding was in agreement with the result given in Figure 14, which showed that the difference between R_p and R_s decreased with increases in sampling frequency.

As shown in Figures 16 and 17, moving from passive to pitting conditions caused an increase in the power level of the current ($-234.2 \text{ dB}_{\text{rms}}/\sqrt{\text{Hz}}$ and $-200.8 \text{ dB}_{\text{rms}}/\sqrt{\text{Hz}}$ respectively) and in the potential ($-142.8 \text{ dB}_{\text{rms}}/\sqrt{\text{Hz}}$ and $-125.3 \text{ dB}_{\text{rms}}/\sqrt{\text{Hz}}$, respectively). In Figure 18, all values of the power level of the current signal calculated from the high-frequencies regions, coming from the same test of Figures 16 and 17, are reported as a function of immersion time. V_c also are reported. An interesting correlation was found between the power level of the current and V_c as shown in Figure 18. The value of the power level at high frequencies has been proposed by some authors to be representative of the corrosion status of the system in the case of pitting attack.¹¹ More recently, the validity of this procedure was confirmed in the case of general corrosion.³⁵ A clear correlation was not found for potential noise. From the ratio of potential and current power level acquired in the frequency domain, it was possible to obtain the power spectral level of the resistance (R_s) according to the Nyquist relationship already reported² and the equivalent one for the current:

$$\bar{I}_n^2 = 4kRT\Delta f / R_s \quad (4)$$

where \bar{I}_n^2 is the mean square noise current.

Figure 19 shows good correlation between R_s and R_p . Differences between R_s and R_p were very small during the whole test in the passive condition and after addition of chlorides.

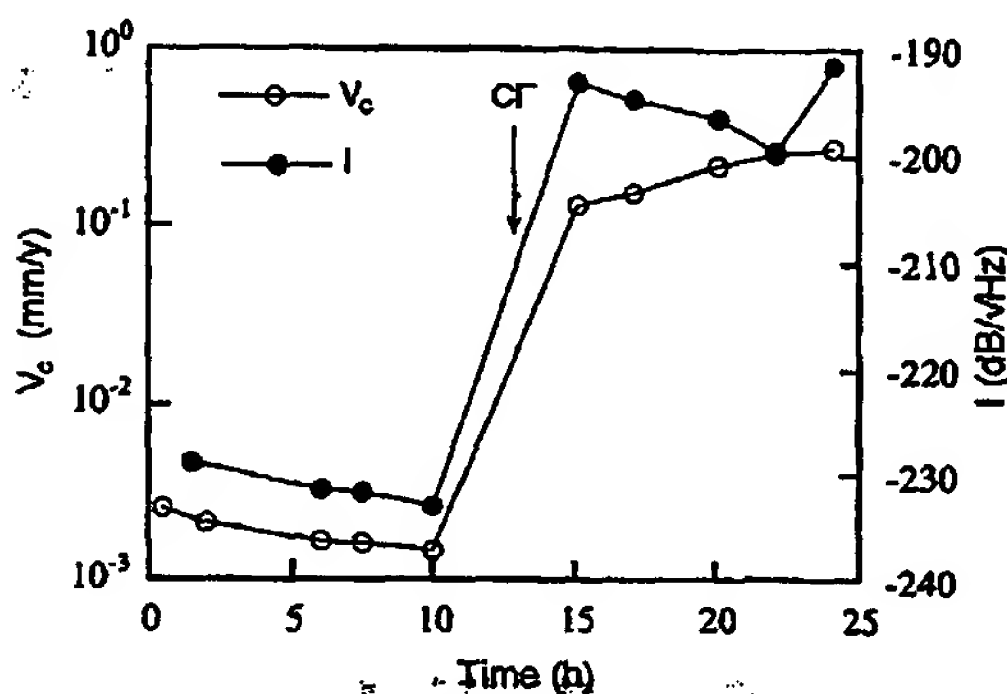


FIGURE 18. Correlation between the power level of the current PSD as calculated from the high frequencies region and the V_c as a function of immersion time (same test as Figures 16 and 17).

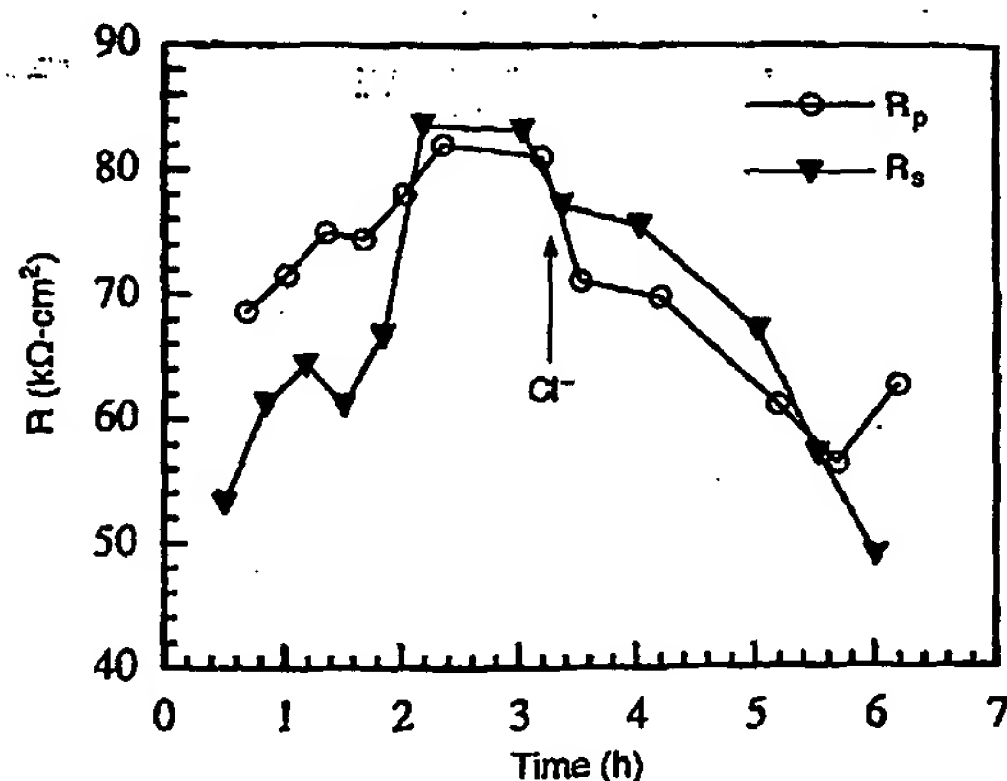


FIGURE 19. Correlation between the power level of the resistance PSD as calculated from the high frequencies region and R_p as a function of immersion time for a 50 mM phosphate solution.

CONCLUSIONS

- ◆ This paper dealt with the feasibility of monitoring a corroding system by using potential and current EN measurements. It was confirmed that, from σ values of the current and potential noises, pitting attack can be revealed at its onset. σ values of the current of ≤ 0.5 nA and σ values of the potential of ≤ 50 μ V characterized the passive state.
- ◆ Good correlation was found between σ of the current data and V_c . The current EN was demonstrated to give more clear information on the corroding system than the potential noise.
- ◆ The signals were processed to obtain R_n . R_n gave values proportional to R_p as measured by LPR, and some quantitative prediction of R_p values from EN data may be possible.
- ◆ EN resistance results were very sensitive to variation of the sampling frequency. High sampling frequencies (32 Hz) gave results closer to the R_p data than ones collected at low sampling frequencies (2 Hz).
- ◆ According to previous findings of other authors, it appears that the rolloff of the PSD plots is characteristic of the corrosion process. A rolloff of ≤ 20 dB/decade in the potential PSD was observed for pitting attack and > 20 dB/decade for the passive condition.
- ◆ From the frequency-independent region of the PSD spectra of the potential and the current noises, the rms value of R_n was calculated. Those values were in good agreement with V_c as calculated by LPR.
- ◆ This study demonstrated that the statistical elaboration of data coming from EN acquisitions under open-circuit condition of two identical electrodes were related to the rate of reaction.
- ◆ In spite of a heavy processing time, R_n appears to be an important tool for predicting V_c with a real nonperturbative detection method. Agreement between R_n and R_p may be very important for theoretical modeling of the nature of the noise of corroding systems.

REFERENCES

1. K. Hladky, J.L. Dawson, Corros. Sci. 21 (1981): p. 317.
2. K. Hladky, J.L. Dawson, Corros. Sci. 22 (1982): p. 231.
3. A.M.P. Simões, M.G.S. Ferreira, Brit. Corros. J. 22 (1987): p. 21.
4. P.C. Searson, J.L. Dawson, J. Electrochem. Soc. 135 (1988): p. 1908.
5. J. Flis, J.L. Dawson, J. Gill, G.C. Wood, Corros. Sci. 32 (1991): p. 877.
6. C. Monticelli, G. Brunoro, A. Frignani, G. Trabarelli, J. Electrochem. Soc. 139 (1992): p. 706.
7. J.B. Lumsden, M.W. Kendig, S. Jeanjaquet, "Electrochemical Noise for Carbon Steel in Sodium Chloride Solution — Effect of Chloride and Oxygen Activity," CORROSION/92, paper no. 224 (Houston, TX: NACE, 1992).
8. G. Gusmano, G. Montesperelli, E. Traversa, "Comparison Between AC Impedance Spectroscopy and Potential Noise Measurements in the Evaluation of Mild Steel Passivation in Cooling Waters," CORROSION/93, paper no. 355 (Houston, TX: NACE, 1993).
9. C. Liu, D.D. Macdonald, E. Medina, J.J. Villa, J.M. Bueno, Corrosion 50 (1994): p. 687.
10. R.A. Cottis, C.A. Loto, Corrosion 46 (1990): p. 12.
11. G. Gusmano, G. Montesperelli, A. D'Amico, C. Di Natale, "Use of Noise Measurements for the Investigation of Corrosion Phenomena," CORROSION/Asia, Singapore, Sept. 26-30, 1994 (Houston, TX: NACE, 1994).
12. R.G. Hardon, P. Lambert, C.L. Page, Brit. Corros. J. 23 (1988): p. 225.
13. D.A. Eden, K. Hladky, D.G. John, J.L. Dawson "Electrochemical Noise — Simultaneous Monitoring of Potential and Current Noise Signals from Corroding Electrodes," CORROSION/86, paper no. 274 (Houston, TX: NACE, 1986).
14. C.-T. Chen, B.S. Skerry, Corrosion 47 (1991): p. 598.
15. U. Bertocci, "Statistics of Localized Breakdown Noise," in Advances in Localized Corrosion, eds. H.S. Issacs, U. Bertocci, J. Kruger, S. Smialowska (Houston, TX: NACE, 1990), p. 127.
16. G.P. Bierwagen, J. Electrochem. Soc. 141 (1994): p. L155.
17. J.F. Chen, W.F. Bogaerts, Corros. Sci. 37 (1995): p. 1,839.
18. P.D. Welch, IEEE Trans. Audio Electroac. 15 (1967): p. 70.
19. W.T. Cochran, J.W. Cooley, D.L. Favon, H.D. Helms, R.A. Kaenel, W.W. Lang, G.C. Maling, Jr., D.E. Nelson, C.M. Rader, P.D. Welch, IEEE Trans. Audio Electroac. 15 (1967): p. 45.
20. U. Bertocci, J. Kruger, Surf. Sci. 101 (1981): p. 608.
21. J.M. Bastidas, S. Feliu, Jr., M. Morcillo, S. Feliu, Prog. Org. Coat. 18 (1990): p. 265.
22. A.K. Livesy, J. Skilling, Acta Cryst. A41 (1985): p. 113.
23. P.R. Roberge, Corrosion 50 (1994): p. 502.
24. G.C. Barker, J. Electroanal. Chem. 21 (1969): p. 127.
25. V.A. Tyagai, Electrochim. Acta 16 (1971): p. 1,647.
26. T. Shibata, Corros. Sci. 31 (1990): p. 413.
27. T. Okada, Corros. Sci. 31 (1990): p. 453.
28. T. Okada, J. Electroanal. Chem. 297 (1991): p. 349.
29. T. Okada, J. Electroanal. Chem. 297 (1991): p. 361.
30. P.J. Brockwell, R.A. Davis, Time Series: Theory and Methods (New York, NY: Springer Verlag, Inc., 1987), p. 14.
31. F.W. Kruse, L.D. McGlauchlin, R.B. McQuistan, in Elements of Infrared Technology: Generation, Transmission, and Detection, 2nd ed., Chap. 7 (New York, NY: John Wiley & Sons, Inc., 1963), p. 236-241.
32. J.C. Uruchurtu, J.L. Dawson, Corrosion 43 (1987): p. 19.
33. J.C. Uruchurtu, Corrosion 47 (1991): p. 472.
34. C. Gabrielli, F. Huet, M. Keddam, R. Oltra, Corrosion 46 (1990): p. 266.
35. A. Legat, V. Dolecek, Corrosion 51 (1995): p. 295.